

Two-dimensional flow patterns near contour grass hedges

Dalmo A. N. Vieira* and Seth M. Dabney

USDA-ARS–National Sedimentation Laboratory, Oxford, MS, USA

Abstract:

Grass hedges are narrow strips of stiff-stemmed vegetation used to control erosion and sediment delivery. When planted on the contour, the hydraulic resistance of the vegetation slows runoff, creates ponding, and promotes sediment deposition. When tillage is performed between grass hedges, soil may be thrown against the vegetation, where it settles to form a berm within the hedge. Tillage-induced berms divert part of runoff, causing it to flow alongside the hedge without crossing it. Such flow partitioning created by grass hedges was measured on experimental plots located on silt loam loess soil near Holly Springs, Mississippi, USA, where hedges planted at the bottom of 5%, 22.1-m-long slopes evolved berms averaging 0.13 m in height. They diverted about 80% of the runoff for events smaller than 5 mm and about 50% for large events. A two-dimensional model was developed to determine overland flow patterns over complex terrains, accounting for oriented roughness created by tillage corrugations, crop rows, and larger features such as berms and vegetative barriers. The model was used to reproduce the flow partition observed in the field experiments and to determine how berm height and slope steepness and length affected runoff redistribution. Numerical simulations indicated that for most runoff events, ponded runoff depths were not high enough to overtop the berm but rather crossed the berms through cracks and gaps, represented in the model as small triangular weirs. The model also was applied to a 6.0-ha watershed in Western Iowa, USA, where nine grass hedges were planted across 12–16% slopes. Computed dynamic flow properties showed that berms increased the amount of runoff flowing laterally upslope of the hedges and that a large portion of the runoff crossed the vegetative strips at a few locations and with high flow depths, increasing the risk of development of ephemeral gullies. Copyright © 2011. This article is a U.S. Government work and is in the public domain in the USA.

KEY WORDS vegetative buffers; grass hedges; runoff; tillage berms; overland flow modeling

Received 10 November 2010; Revised 14 January 2011

INTRODUCTION

Grass hedges are narrow strips of stiff vegetation planted on elevation contours as a soil conservation and water resource protection measure. The hydraulic resistance created by the vegetation increases overland flow depths and creates temporary ponded areas upslope of the hedges, slowing runoff and promoting deposition of eroded sediment (Dabney, 2003; Dabney *et al.*, 2009). In areas of concentrated flow, grass hedges may help slow and spread runoff, protecting downslope areas against the formation of ephemeral gullies. As a result of the flow ponding, grass hedges usually redirect part of the runoff to flow laterally along the upper edge of the hedge, modifying surface flow patterns.

When tillage is conducted near these hedges, soil can be thrown against the vegetation and deposited next to it. Depending on tillage implement characteristics and on the proximity of the first tillage pass next to the vegetation, a berm may or may not form within the hedge (Vieira and Dabney, 2011). If such a berm does form, it creates a ‘berm and grass hedge barrier’ (BGHB) that may prevent water from entering the vegetated area and cause a larger portion of runoff to be diverted, running laterally alongside the

hedge. Such flow will accumulate on the upslope side of the BGHB until there is a gap or a low point (such as where the hedge line crosses a swale) that allows the runoff to cross the BGHB. Field experiments conducted on 0.1-ha plots near Holly Springs, Mississippi, USA, indicated that grass hedges significantly decreased erosion and that, when berms were present, about 85% of the runoff for small events, and 55% for large events, flowed laterally above rather than through the hedges (Dabney *et al.*, 2011).

A two-dimensional (2D) overland flow model was developed to specifically account for the impact of oriented roughness created by tillage furrows, crop rows, and larger scale features such as berms and vegetative barriers on runoff flow patterns. In this work, the 2D model was used to investigate how grass hedges and associated tillage-induced berms affect the distribution of runoff and to reproduce field observations from a plot study conducted in North Mississippi. The model also was used to investigate how berms modify flow patterns and runoff redistribution in a 6-hectare field at Treynor, Iowa, USA, where nine lines of grass hedges were planted approximately on the contour across 12–16% slopes.

2D OVERLAND FLOW MODEL

Oriented roughness

Overland flows resulting from natural events are characterized by rapidly changing flow rates and water depths as

*Correspondence to: Dalmo A. N. Vieira, USDA-ARS–National Sedimentation Laboratory, P.O. Box 639, State University, AR 72467, USA.
E-mail: dalmo.vieira@ars.usda.gov

runoff concentrates in swales and depressions during a storm, resulting in a flow field that is highly variable in both space and time. The development of flow patterns is determined by the unsteadiness and spatial variability of runoff, topographic characteristics that determine flow concentration and accumulation, and the hydraulic resistance associated with the diverse ground surfaces found in the agricultural landscape.

Surface roughness is usually anisotropic, with directions of high and low hydraulic resistance caused by oriented roughness created by tillage corrugations and wheel tracks, and by larger-scale features such as crop rows (ridges and furrows), vegetative barriers, and tillage-induced berms. As runoff flows along the direction of least hydraulic resistance, its flow path is not necessarily along the steepest slope but in the direction that results from the interaction of terrain steepness and hydraulic resistance.

Flow patterns are complex because local flow directions are dependent on flow depths that rise and fall during the runoff event and vary significantly in space because of flow concentration created by the topography. For small flow depths, runoff flows preferentially in the direction of least resistance, but when flow depths increase, runoff tends to align with the direction of the steepest slope. Therefore, overland flow patterns are not determined exclusively by topography but rather from a combination of local terrain slope steepness and how height and orientation of roughness elements relate with flow depth.

Governing equations

To reproduce and predict dynamic flow patterns, the Two-dimensional Overland Routing of Runoff Events (TORRENT) model was developed to use high-resolution terrain data to represent fine scale topographic features. The model is based on the principles of conservation of mass and momentum and simulates unsteady flows to account for the high variability of flow properties during the progression of runoff events. The diffusive wave approximation was used, providing computational efficiency, accuracy, and stability (Vieira, 1983) while allowing the computation of backwater effects caused by obstructions created by topography, vegetative barriers, and so on. The conservation of mass and momentum in two dimensions are defined by the following relationships (Abbott, 1979):

$$\frac{dh}{dt} + \frac{\partial q_x}{\partial x} + \frac{\partial q_y}{\partial y} = r_o, \text{ and} \tag{1}$$

$$\begin{cases} \frac{dH}{dx} + S_{fx} = 0 \\ \frac{dH}{dy} + S_{fy} = 0 \end{cases} \tag{2}$$

where h is the water depth, H is the water surface elevation, q_x and q_y are flow discharges in the Cartesian directions x and y , r_o is the net runoff (volume of runoff per unit area per unit time), and S_{fx} and S_{fy} are components of the friction slope \vec{S}_f , the slope of the total energy line that represents energy dissipated because of surface resistance.

Anisotropic hydraulic resistance

Many overland flow models have been developed in the past using either the kinematic or the diffusive wave assumptions (e.g. Gottardi and Venutelli, 1993; Tayfur *et al.*, 1993; Di Giammarco *et al.*, 1996; Defina, 2000; Brufau *et al.*, 2002; Liu *et al.*, 2004). The vast majority of these models assumed that hydraulic roughness is isotropic, that is, independent of the flow direction. However, for flows over agricultural fields, it is important to consider the presence of oriented roughness. Strelkoff *et al.* (2003) presented a derivation of the 2D flow equations, assuming hydraulic roughness is defined for two orthogonal axes along which the roughness coefficients have their maximum and minimum values. The same reasoning was applied to the Precision Agricultural Landscape Modeling System (PALMS) model (Molling *et al.*, 2005).

In following the derivation by Strelkoff *et al.* (2003), the flow discharge over a point on the terrain is defined as the vector $\vec{q} = K\sqrt{S_f}$, where K is the conveyance. In the case of anisotropic roughness, K is a tensor with principal directions of maximum and minimum conveyance. In using Equation (2), flow discharges over the terrain can be written as components along the Cartesian directions x and y :

$$\begin{bmatrix} q_x \\ q_y \end{bmatrix} = -\frac{1}{G} \begin{bmatrix} K_{xx} & K_{xy} \\ K_{yx} & K_{yy} \end{bmatrix} \begin{bmatrix} \partial H/\partial x \\ \partial H/\partial y \end{bmatrix} \tag{3}$$

where $G = [(\partial H/\partial x)^2 + (\partial H/\partial y)^2]^{1/4}$. The conveyance tensor components are as follows:

$$\begin{aligned} K &= \begin{bmatrix} K_{xx} & K_{xy} \\ K_{yx} & K_{yy} \end{bmatrix} \\ &= \begin{bmatrix} K_A \cos^2\theta + K_B \sin^2\theta & (K_A - K_B) \sin\theta \cos\theta \\ (K_A - K_B) \sin\theta \cos\theta & K_A \sin^2\theta + K_B \cos^2\theta \end{bmatrix} \end{aligned} \tag{4}$$

where $K_A = \frac{1}{n_A} h^{5/3}$, $K_B = \frac{1}{n_B} h^{5/3}$, and θ is the counterclockwise angle between the x -axis and the line \vec{r} defining the local roughness orientation (Figure 1). The Manning's coefficients n_A and n_B define the minimum and maximum flow resistance in orthogonal directions parallel and perpendicular to the direction given by the line \vec{r} . Equation (3) is combined into Equation (1), which is then discretized using the finite volume method with a uniform grid of square cells, resulting in a set of algebraic equations relating water elevations at the centre of each computational cell (Figure 1a) to those at the four neighboring cells (N, S, E, and W).

In the case of isotropic resistance, the vectors \vec{q} and \vec{S}_f are collinear and oriented in the direction of the steepest descent of the water surface. If flow resistance is anisotropic, the flow vector \vec{q} deviates from the direction of \vec{S}_f towards the direction of least resistance \vec{r} (Figure 1b), and its direction and magnitude are determined by Equation (4). In the model, complex patterns of oriented roughness, such as those created by the curvilinear paths of contour tillage, are described by the orientation angle θ and the Manning's coefficients n_A and n_B , specified for each computational cell. The coefficients n_A and n_B are not constant but rather are function of the local flow conditions.

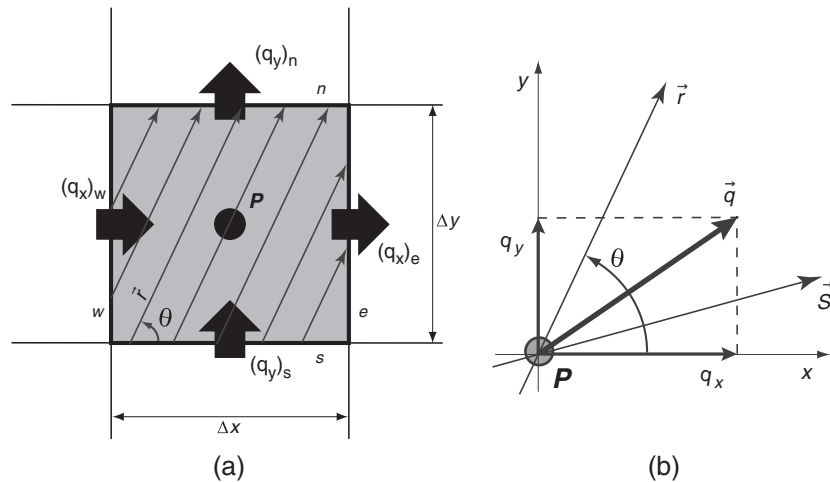


Figure 1. (a) Typical control volume used by the overland flow model. Flow properties are computed at the center point P. Flow discharges are computed at the element faces for each time step. Lines indicate the direction of least hydraulic resistance for the control volume. (b) The direction of the resultant flow discharge for the control volume is indicated by the vector \vec{q} , for which q_x and q_y are the components in the Cartesian directions. In the case of anisotropic roughness, the flow direction deviates from the direction of the friction slope \vec{S}_f towards the direction of least resistance \vec{r} , defined by the angle θ

This allows computed flow directions to respond to relative changes in surface roughness resulting from varying flow depths.

The system of equations is solved using the strongly implicit procedure of Stone (1968). Simulations start with a dry surface, and flow depths and discharges are computed for the duration of the runoff event in a series of time steps. Time step sizes are chosen as a function of grid size and flow depths. Even if the implicit solution scheme produces a stable solution when larger time steps are chosen, the use of small time steps ensures conservation of mass when flow depths are very small (Lal *et al.*, 2010). Because the numerical solution can lead to negative water depths, a minimum water depth (on the order of 0.1 mm) is enforced. Also, when the bed of a particular cell is drying, discharges leaving the cell are limited according to the volume of water still available in the cell, preserving conservation of mass. Two types of boundary conditions are implemented in the model: a non-reflective open boundary condition specified at the edges of the simulation domain that allows water to leave without affecting the flow in the interior and a closed boundary condition that blocks the flow across lines specified by the user.

Roughness coefficients

Hydraulic resistance is a combination of random roughness that is a function of soil clod sizes and their distribution over the terrain, oriented roughness created by tillage, crop residue cover, and drag created by vegetation at different degrees of submergence. In this model, the Manning's coefficients n_A and n_B define the hydraulic roughness in the directions of least and most resistance, respectively. These coefficients not only account for the anisotropy of microrelief, but they also can be used to represent blockage created by subgrid-scale features, such as the ridge and furrow pattern of crop rows. The specification of a large n_B indicates higher resistance across the rows and results in most flow being conveyed along the furrows.

Experiments have shown that the roughness coefficients are not constant with flow depth and that values of Manning's n may vary by an order of magnitude or more for depths commonly found in overland flows. The presence of macroscale roughness leads to a non-monotonic relationship between resistance and depth (Temple and Dabney, 2001; Dabney, 2003). When flow depths are not large enough to submerge all roughness elements, resistance increases as drag increases with depth. In the case of stiff vegetation, the drag created by stems is practically negligible for small depths but rapidly increases when a larger surface area is exposed to the flow, reaching a maximum value near the point of complete submergence. For flexible vegetation, frictional resistance decreases as submergence increases. For overland flows, it is important that flow resistance be determined as a function of local flow conditions, as flow depths over an agricultural field may vary substantially. Empirical data relating Manning's n and flow conditions are available from laboratory and field experiments for a variety of surfaces (e.g. Gilley and Kottwitz, 1993; Temple and Dabney, 2001). Such data must be used to define how n_A and n_B change with flow depth, and such relationship may be supplied to the model as tabulated curves. Alternatively, established relationships between n and flow properties have been implemented in the model (Temple *et al.*, 1987; Gilley *et al.*, 1991; Gilley and Kottwitz, 1993; Wu and Wang, 2004).

Permeable barriers

Agricultural landscapes are frequently covered with microtopographic features, created either by tillage and seedbed preparation or through erosion and deposition by wind and water. Crop rows, terrace walls, and tillage-induced berms are examples of barriers that are capable of substantially diverting surface flows, especially shallow flows. However, such barriers may not be completely impervious to water; their variable heights may allow partial overtopping, and they are rarely continuous because

of damage by mechanical action and water erosion. To simulate the hydraulic behavior of these barriers, a mechanism was implemented in the flow model to allow the controlled passage of water through the barrier. The approach assumes that the flow rate across the permeable barrier increases with increasing local hydraulic head, computed by the model during the development of the runoff event. Flow rates across the barrier are determined based on the hydraulics of triangular (v-notch) weirs. The magnitude of flow rate (per unit length of barrier) can be controlled by a set of parameters (described below) that define the hydraulic characteristics of the barrier so that it responds to the varying flow conditions in the vicinity of the barrier during the development of a runoff event. These parameters are determined through calibration using field information, but once determined, the model can compute discharges across the barrier for flow conditions created by storm events of different magnitudes, also considering the changes in water depths upslope of the barrier created by flow concentration because of topography, or backwater effects created by the barrier itself.

In TORRENT, barrier permeability is controlled by a series of small triangular slits distributed along the barrier, as illustrated in Figure 2; their number, distribution, and size control the flow rates as a function of the constantly varying flow depth next to the barrier. Slits are grouped in sets, and each set has slits with vertices at different elevations, so the response of discharge to hydraulic head can be better controlled. The overall flow discharge can be adjusted by the notch angle ϕ , and the use of multiple small openings allows a more uniform distribution of flow rates along the barrier. For example, if water accumulates at a low point along the barrier, more slits are activated, and larger flows cross the barrier at that location.

Flow discharges across the barrier are determined by an empirical equation derived for flows through triangular weirs (Chow, 1959):

$$q_{si} = \frac{8}{15} C_d \sqrt{2g} \tan\left(\frac{\phi}{2}\right) H_{si}^{5/2}, \quad (5)$$

where q_{si} is the discharge through a particular slit i , C_d is the discharge coefficient, g is the acceleration of gravity, ϕ is the slit angle, and H_{si} is the hydraulic head at that slit. This equation establishes the relationship between flow discharge and flow depth in the upslope side of the barrier,

but it is not expected to be an accurate predictor of overall flow rate through the barrier. Calibration using field measurements is required, which can be accomplished by defining the number of slits in a set, the spacing of slit sets along the barrier, and controlling the vertical distribution of slit vertices within a slit set.

The position of each slit set relative to the cells in the 2D domain is known, so the flow discharges for all slits located in a 2D cell are added to determine the total flow discharge through the barrier for that cell. This discharge is added or subtracted to the net runoff [r_o in Equation (1)] for the corresponding 2D cells where water enters or leaves through the permeable barrier.

Model inputs

Input data for the overland flow model are prepared with the help of the GIS software. Terrain elevation is given in the form of a digital elevation model (DEM), which also defines the grid resolution used in the computations. GIS layers also define zones with the same roughness parameters (representing different managements such as cropland, vegetative buffer, grassed waterway, etc.), directions of oriented roughness (the direction of least hydraulic resistance is given at the center of each raster cell), and the location of permeable barriers (defined as line segments overlaying the DEM). Runoff rates can be specified as time series corresponding to different zones in the simulation domain. Other data are provided in a master XML file that includes model options and parameters, additional input files, boundary types and locations, roughness coefficients for the several roughness zones, and discharge parameters for the permeable barriers.

MODEL SIMULATIONS

Simulation of runoff patterns in the Holly Springs plots

Field description. The effects of grass hedges on runoff reduction and/or redirection and on sediment trapping were studied on a set of four 0.1-ha plots located on shallow loess soils near Holly Springs, Mississippi (Dabney *et al.*, 2011). In two of the plots, switchgrass (*Panicum virgatum* L.) hedges 1.0 m wide and 45 m long were planted along the bottom end of a 22.1 m long 5% slope, just above a concrete channel that gathers and conveys any runoff flowing

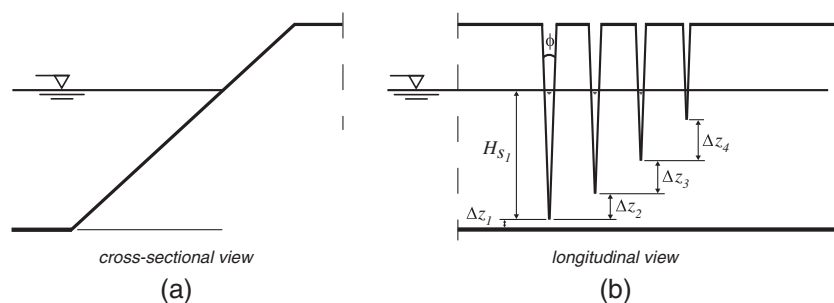


Figure 2. Sketch of an idealized permeable barrier: (a) cross-sectional view and (b) longitudinal view showing a set of discharge slits. Flow across the barrier is controlled by the number of slits, the notch angle ϕ , and the vertical positioning of the slit vertices

through the hedges, as shown in Figure 3a. All plots were built with a 0.3% cross-slope grade, and measuring flumes and sediment samplers were installed to collect and record runoff coming from both the upslope and downslope sides of the hedges.

The plots were planted to corn (*Zea mays* L.) on exact contour, so the rows were not quite parallel to the grass hedge with its 0.3% grade. A tillage-based management consisting of disking, chisel plowing, and harrowing was used from 1996 to 2000, with care being taken so that soil clods were not thrown against the hedge and that any furrows formed next to the hedges were smoothed by harrowing. Starting in 2001, tillage was moved closer to the hedge, and soil deposited against the hedge was left in place, resulting in the formation of a BGHB. Annual tillage operations gradually increased the berm height, which reached an average of 0.13 m by 2004, when the study was concluded. Figure 3b shows the average slope profile and the tillage berm.

Analysis of runoff data collected from all the plots indicated that, as expected, the introduction of the grass hedges reduced runoff and sediment yield and that the formation of a BGHB greatly altered runoff flow patterns (Dabney *et al.*, 2011). When berms were not present, runoff passed through the hedges into the concrete channel, and very little flow was diverted by the hedges. In contrast, when a BGHB was formed, most of the runoff was diverted to flow parallel to and upslope of the BGHB, leaving the field without crossing it. Measurements also

showed that the fraction of flow diverted by the BGHB varied with the magnitude of the field runoff. For smaller events, most of the runoff was diverted, whereas for larger events, water that accumulated behind the BGHB provided the hydraulic head for the water to cross it at flow rates that increased with the size of the runoff event. Dabney *et al.* (2011) determined that the portion of runoff diverted by the BGHB could be described by $R_d = 0.9R^{0.89}$, where R_d is the runoff flowing laterally upslope of the BGHB, and R is the total event runoff (both in millimetres).

Model set-up. The geometry of the 0.1-ha plots was defined for the flow model simulations by a rectangular mesh of 0.20-m resolution. The area near the slope bottom comprising the concrete channel and the BGHB was described by an average profile based on field measurements taken in 2004. The remainder of the field was assumed to be planar with a 5% slope towards the concrete channel and a 0.3% lateral slope parallel to the channel. Hydraulic roughness for the cropped area was specified as Manning's $n = 0.04$ along the crop rows, which are aligned with the terrain contours, and $n = 0.08$ in the direction normal to crop rows. The flat area just upslope of the BGHB (about 0.6 m wide) that was covered by grass clippings and accumulated litter was assigned a constant Manning's n of 0.2, whereas a value of 0.8 was used for the part covered by the BGHB.

To evaluate the influence of the BGHB on the distribution of runoff for events of varied magnitudes,

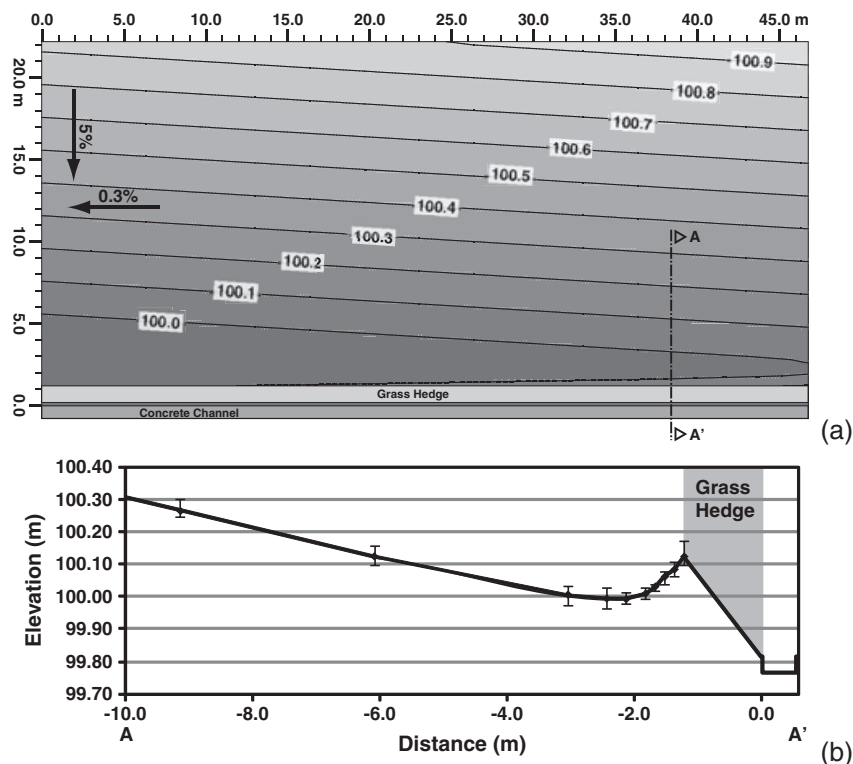


Figure 3. (a) Plan view of a typical 0.1-ha plot near Holly Springs, Mississippi, USA (elevation contour lines in meters), where a 1.0 m-wide grass hedge was established at the bottom of a 5% slope. (b) Cross-sectional profile showing the grass hedge, tillage-induced berm, and concrete channel for collection of runoff. The black line indicates the averaged surveyed elevations, and error bars show the range of deviations from the average elevation (after Vieira and Dabney, 2011)

computed runoff that collected upslope of BGHB and left the plot towards the grass waterway was compared to runoff that crossed the BGHB and flowed in the concrete channel. Infiltration was not simulated; instead, net constant runoff was specified. Each simulation started with the nominal water depth assumed by the model. Water gradually flowed towards the slope bottom, and flow depths gradually increased upslope of the BGHB. Computed flow discharges leaving the plot from each side of the BGHB were compared after 1 h of continuous runoff.

Permeable barrier. Preliminary model tests showed that when flow depths at the bottom of the plot were small, the berm geometry completely blocked runoff trying to cross the grass hedge. Overtopping was only possible for large events and was usually restricted to the section of the berm near the lower part of the plot, where runoff from the entire field accumulated above the berm just before it left the plot. Therefore, the BGHB was defined in the model as a permeable barrier, with flow discharges across the barrier being governed by Equation (5). A series of calibration simulations were conducted to determine the optimum set of parameters so that the fraction of total runoff being diverted by the berm would match field measurements for runoff intensities between 5 and 75 mm/h. First, the number and notch angle of discharge slits were adjusted to control the flow crossing the berm for the full range of runoff events. The calibration was then fine-tuned by adjusting the vertical distribution of the slit vertices; the increment in the elevation of the slit vertices was determined using a logarithmic function so that the model would respond better to changes in flow depths near the berm and correctly reproduce the observations. The modelled and measured flow partitions created by the berm, expressed as the fraction of the runoff diverted and flowing upslope of the berm to the total runoff, are compared in Figure 4. The agreement between computed and measured flow partitions was obtained using sets of four triangular slits of 2.5° notch angle, with the first slit in each set $\Delta z_{s(1)} = 0.01$ m above

the ground and subsequent slit vertices placed higher at variable elevation increments defined by $\Delta z_{s(i+1)} = \ln(i+1)\Delta z$, $i = 1, 2, \dots$ with $\Delta z = 0.01$ m (Figure 2).

Hydraulic behavior. Model simulations showed that, for the plot dimensions and berm heights observed in Holly Springs and assuming the BGHB to be completely impervious, the BGHB diverted 100% of the plot runoff for all events smaller than 50 mm/h. Because of the berm height (0.13 m) and the small slope length (22.1 m) of the experimental plot, only large events were capable of generating water depths behind the berm that could overtop the berm and flow through the grass hedge. However, for events of any size, runoff gradually collected upslope of the BGHB and flowed laterally towards the lower side of the plot without crossing the BGHB. Flow depths increased along this lateral path towards the plot edge because of the increased flow contribution from the entire plot.

Influence of berm geometry on flow diversion. To determine how flow is diverted by tillage berms, model simulations were set up for configurations similar to those of the Holly Springs experimental plots: a single 1.0 m-wide grass hedge atop a triangular-shaped berm at the bottom of the slope, with the permeability properties as deduced from field measurements. The 2D model was used to compute the fraction of surface flows diverted by grass hedges with different berm heights (2, 4, 8, and 13 cm), for hedges established on plots of different slope lengths (22, 50, and 100 m) and steepnesses (2.5, 5, 10, and 15%). Each plot configuration was tested with runoff events of different magnitudes (5, 25, and 50 mm/h). To facilitate comparison, all flow characteristics were analysed at 1 h after the beginning of runoff, when flow discharges had reached steady state and discharges crossing and being diverted by the BGHB were easily determined.

The berm height was the primary factor determining the portion of runoff that was diverted by the BGHB. Figure 5 shows the fraction of the total runoff diverted by a berm at the bottom of a 22-m slope of 5% steepness. The diversion

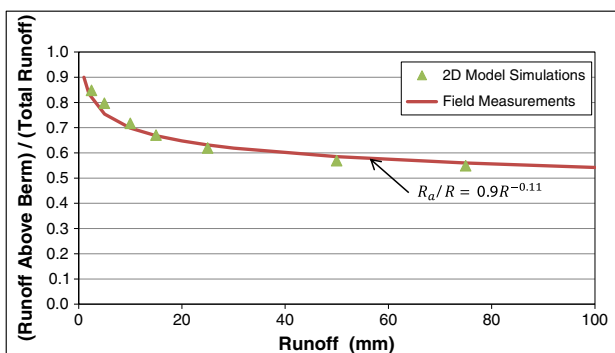


Figure 4. Fraction of the total runoff that flows upslope of the grass hedge, for runoff events of different magnitudes. The solid line represents the runoff partition relationship deduced from field measurements (Dabney et al., 2011), and the symbols show the partition obtained with two-dimensional model simulations

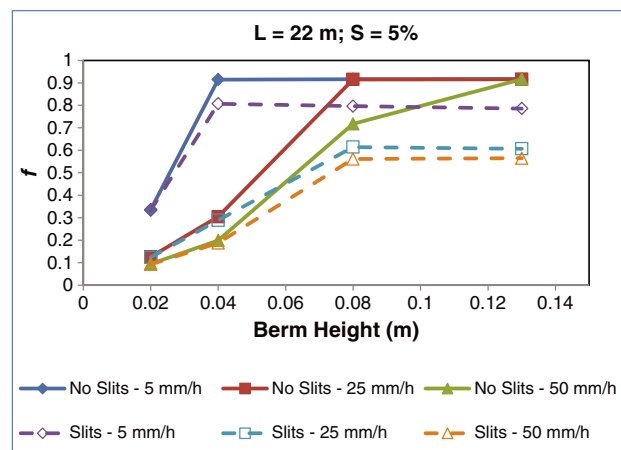


Figure 5. Partition of runoff created by berm and grass hedge barrier. The fraction f is defined as the ratio of runoff flowing laterally above the barrier to the total runoff for the event

fraction f is computed as the runoff leaving the plot above the berm divided by the total runoff from the plot. Diversion fractions are shown assuming the berm to be permeable (with ‘slits’) and completely impervious (‘no slits’). For the 13 cm-high berm, water accumulated upslope of it did not reach depths sufficient to overtop it. The fraction of runoff percolating through it was larger for events of larger intensity because water depths near the berm also were larger. For berms of lower heights (2 and 4 cm), overtopping was more frequent, and a much larger fraction of runoff flowed over the berm and through the vegetation.

The second geometric factor was the length of the plot. A larger area contributing runoff towards the hedge resulted in higher water depths and more runoff crossing the hedge. Figure 6 shows the runoff partition for different berm heights and runoff event sizes.

Slope steepness has a dynamic effect on flow depths developing during the rising and receding phase of a hydrograph. An increase in terrain steepness facilitates the crossing of field roughness such as tillage corrugations, resulting in smaller flow depths over the cropped area and slightly higher depths near the hedges. Model computations showed that more runoff crossed the hedges when the plot was steeper, but this effect was small.

Simulation of flow patterns across contour grass hedges

Field description. A 6.0-ha watershed near Treynor, Western Iowa, USA, has been used as an experimental field for numerous hydrological and erosion studies (e.g. Alberts *et al.*, 2001; Ghidey *et al.*, 2001; Wilson *et al.*, 2003; Rachman *et al.*, 2008). The watershed is located on deep loess soils and has side slopes of 12–16%. It has been cropped primarily to continuous corn using conventional tillage practices. A series of nine stiff grass hedges were

planted on the contour in 1992, approximately 1.0 m wide and 15 m apart. In the spring of 1999, a detailed real time kinematic (RTK) GPS terrain survey was conducted. Terrain elevations were gathered from both sides of each grass hedge. Figure 7 shows the watershed, which is commonly referred to as W-11. The surveyed elevation points were used to define a triangular irregular network from which a DEM with 0.5-m resolution was created using linear interpolation. The derived terrain surface shows that water and tillage erosion reduced the slope steepness in the areas between grass hedges and that terrace benches started to form. The surface also includes swales that are scars of past erosion, where older gullies used to cut across the location of the grass hedges and converged at the top end of the grassed waterway leading to the watershed outlet.

Model set-up. Hydraulic roughness for the cropped areas between the hedges was specified assuming that the least resistance was along the lines parallel to the grass hedges. GIS scripts were used to determine roughness orientation angles for each cell in the DEM, interpolated from the orientation of nearby hedge lines. Manning’s n coefficients of 0.03 and 0.08, assumed to be independent of flow depth because flow depths are very small, represent the oriented roughness created by tillage and crop rows. For the stiff grass hedges, roughness coefficients were specified to vary with flow-specific discharge, according to the curve in Figure 8, which is a composite of experimental data from several sources (Temple *et al.*, 1987; Dabney, 2003). Resistance coefficients for the grassed waterway were computed using the formula by Temple *et al.* (1987) and reflect reduced Manning’s coefficients with increased submergence.

Influence of tillage berms. A constant, uniform runoff intensity of 50 mm/h was specified over the entire

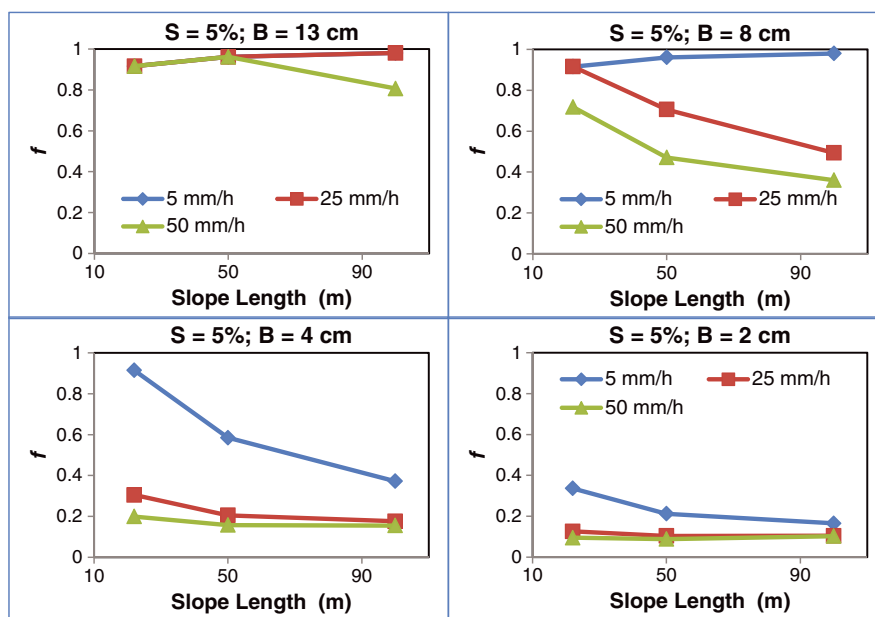


Figure 6. Flow partition as a function of the length of terrain slope above the barrier, for berm heights of 13, 8, 4, and 2 cm and runoff events of 5, 25, and 50 mm/h

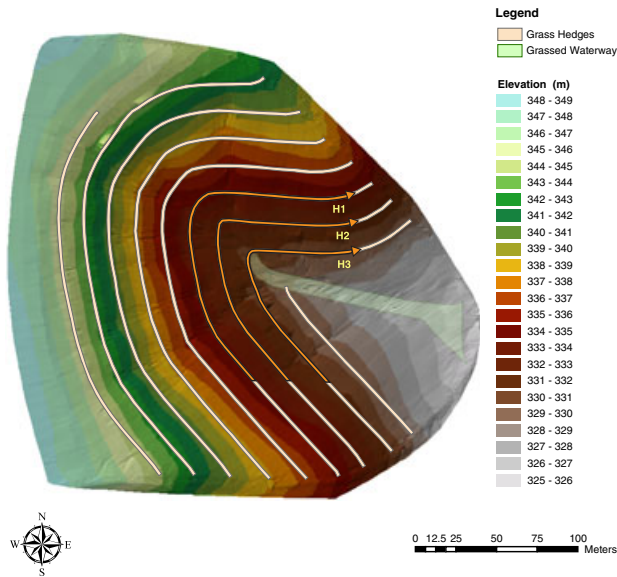


Figure 7. Watershed W-11 near Treynor, Iowa. Colors indicate terrain elevations in meters. Grass hedges were planted nearly on the contour, spaced at 15-m intervals. Grass hedge sections identified as H1, H2, and H3 are used in Figure 10

watershed. The TORRENT simulation started with dry terrain, and flow discharges and depths were computed using a 1.0 s time step. Figure 9a shows computed water depths at 1 h after the beginning of runoff. Resistance created by grass hedges caused larger flow depths in the upslope parts of the hedges, but substantial amounts of runoff crossed the hedges. The development of ephemeral gullies in the past created eroded areas that were not completely refilled with soil by tillage, forming swales that crossed the hedges. At these locations, water accumulated and crossed the hedges at high flow rates.

The same simulation was repeated on a modified DEM where terrain elevations were raised by 0.15 m at the location of grass hedges to simulate the presence of small berms similar to those observed in the Holly Springs experimental plots. The berms were assumed impervious; flow crossed the berms by overtopping them at locations of concentrated flow. Water depths depicted in Figure 9b show how the flow was diverted by the berms; now, a substantial part of the runoff runs parallel to the hedges until it reaches the swales that were created by past erosion.

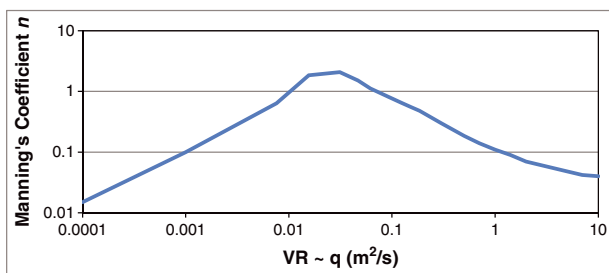


Figure 8. Manning's roughness coefficients as a function of specific flow discharges for stiff switchgrass (*Panicum virgatum* L.) hedges, as implemented in the numerical model, based on experimental data reported in Temple *et al.* (1987) and Dabney (2003)

Water accumulates at these lower points, where depths of up to 0.3 m or more can be observed. For these flow conditions, the influence of the stiff vegetation on hydraulic resistance is important, and values of Manning's n , determined by the curve depicted in Figure 8, change from about 0.015, where depths are small, to near 2.0, where concentrated flows cross the hedges. Figure 10 illustrates how water depths and hydraulic resistance created by the vegetation vary along the three representative hedge segments identified in Figure 7.

The computed flow patterns show how the grass hedges create areas of backwater that slow down runoff and provide an opportunity for sediment to be deposited. However, these areas of increased hydraulic head also are locations where a possible rupture of the BGHB may occur, with the resulting concentrated flow through the barrier possibly leading to the formation of an ephemeral gully. From the simulation, we also see that the grass hedges towards the bottom of the slope receive more runoff but that the overall flow distribution is irregular because fine details in the topography determine how flow concentrates into existing swales. This model application to a real field brings the history of past erosion into play, which is recorded in the topography and continues to influence how runoff concentrates at certain locations, reinforcing past patterns of erosion. It also exemplifies how complex flow configurations develop and are influenced by small topographic features; when tillage berms are present, water concentrates before crossing the hedge, changing flow patterns considerably.

DISCUSSION AND CONCLUSION

Measurements and model simulations indicated that the modified terrain near a grass hedge created by water and tillage deposition is the primary factor in diverting water that otherwise would cross the grass hedge. Although the hydraulic resistance created by the vegetation significantly increases water depths upslope of the hedge and creates an area of backwater (Meyer *et al.*, 1995; Dabney *et al.*, 2009), this happens primarily for large runoff events or at locations where flow is already concentrated as a result of topography. When flow depths are small, the drag created by the vegetation is usually not large enough to modify flow conditions significantly, but just a small berm of deposited soil or accumulated litter along the hedge can be enough to significantly reduce the amount of water crossing the hedge.

Grass hedges implemented in agricultural fields may not perform as expected because, often, runoff is diverted and collected at points of lower elevation, thus creating preferred crossing locations. Field experiments showed that if tillage-induced berms are allowed to develop, the raised elevation created by soil deposition on the upslope side of the grass hedges blocks runoff from ever reaching the vegetation, with a large fraction of the total runoff being diverted. Experiments also showed that hedges are permeable and that the fraction of runoff that crosses it increases non-linearly with runoff rate. Even if water

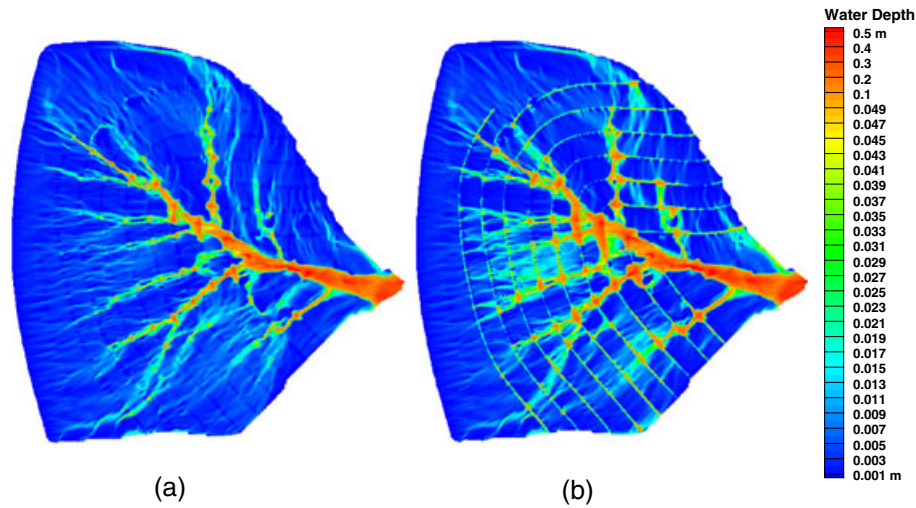


Figure 9. Computed water depths for watershed W-11 near Treynor, Iowa. (a) Field with grass hedges and (b) grass hedges with an associated 15-cm berm. Areas of backwater are created above the hedges where flow concentrates at low points along the hedge. When berms are present, runoff is blocked, and a larger part of runoff is diverted to flow along the hedges, increasing flow concentration at locations of past erosion

depths in the upslope side of the berm do not allow overtopping, the natural berm permeability caused by variations in berm height, cracks, and gaps, and created by decaying vegetation, animal burrows, and other types of damage, allows water to cross. In order for the numerical model to reproduce the observed behavior, flow across the berm and hedge was assumed to be proportional to the available hydraulic head. The use of simulated triangular slits that allow more flow to pass with higher flow depths, combined with the approach in which more pathways become active when water depths are higher, allowed the model to provide a good match to measured data for a wide range of runoff events. Although the method requires calibration, it provides a good description of the hydraulic behavior observed in the experimental plots.

Model simulations indicated that, for the combination of relatively small plot sizes and high berm heights found on the Holly Spring plots, overtopping of the berm and flow through the hedge rarely occurred. When the berms were assumed impervious, model simulations indicated that even a low berm diverted a substantial amount of runoff, particularly for events of lesser intensity. Tests with longer slope lengths showed that more runoff accumulates near the grass hedge, facilitating overtopping. Therefore, larger plots result in larger fractions of runoff crossing the hedge, as the hedge collects more runoff. This is analogous to the situation where a series of hedges are placed on a long slope; runoff crossing the top hedges also contributes to the water flows at the hedges near the bottom, resulting in larger flow depths and easier overtopping with each subsequent hedge downslope.

Model simulations with different slope steepnesses indicated that the fraction of runoff that crossed the hedge was slightly larger for steeper slopes. Model results indicated that, for milder slopes, water depths over the entire plot were higher, resulting in smaller water depths near the hedge.

The application of TORRENT to the small watershed near Treynor, Iowa, illustrated that the use of the model

with actual complex topographic data gives insight on how runoff flows are distributed over the field. The relief created by past erosion partially controls how flow concentrates over the terrain. The hydraulic resistance associated with the grass hedges creates areas of backwater that can promote deposition of eroded sediment. However, these areas are limited to locations where runoff is already concentrated by the topography, as only at these locations does the vegetation provide hydraulic resistance to create ponding. Elsewhere, flow depths are small, and the stiff vegetation does not add much to flow resistance.

When it was assumed that a small berm was present alongside the hedges, the flow computation showed how water was easily diverted to flow laterally behind the berm

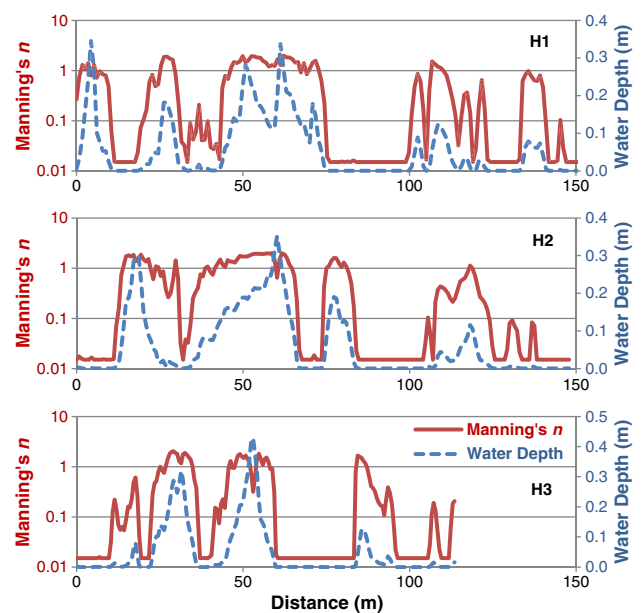


Figure 10. Water depths and Manning's roughness coefficients along the three grass hedge stretches, H1, H2, and H3, shown in Figure 4, for flow conditions shown in Figure 9b (test with 15-cm berms, 1h after the initiation of runoff)

and then concentrate within the swales. This added accumulation can possibly reinforce the erosion process, as past erosion recorded in the topography facilitates flow concentration, resulting in larger flow depths and increased erosivity. However, if grass hedges are well established and do not fail under high flows, backwater created by the hedges can induce sediment deposition so that the swales are gradually refilled with sediment; runoff is then better redistributed over the terrain, reducing flow concentration and the risk of damage to the grass hedges.

Both field observations and model simulations show that flow characteristics near grass hedges can be easily affected by tillage berms. On flat lands, berms may dominate surface drainage patterns, with impacts on soil and water conservation that can be either beneficial or detrimental. Grass hedges are efficient in retarding and dispersing runoff, thereby protecting the slope below the hedge, but unplanned flow diversion and concentration may exacerbate erosion and lead to the development of ephemeral gullies. Management of grass hedges should include periodic inspections and maintenance to ensure that the formation of tillage berms or damage to the vegetation do not create adverse flow conditions that may reduce their effectiveness as an erosion control measure.

REFERENCES

- Abbott MB. 1979. *Computational Hydraulics – Elements of the Theory of Free Surface Flows*. Pitman: Boston; 326.
- Alberts EE, Kramer LA, Ghidey F. 2001. Sediment deposition within a watershed with stiff-stemmed grass hedges. In *Soil Erosion Research for the 21st Century: Proceedings of the International Symposium, 3–5 January, 2001, Honolulu, Hawaii, USA*, Ascough II JC, Flanagan DC (eds). American Society of Agricultural Engineers: St. Joseph; 167–170.
- Brufau P, Garcia-Navarro P, Playan E, Zapata N. 2002. Numerical modeling of basin irrigation with an upwind scheme. *Journal of Irrigation and Drainage Engineering* **128**: 212–223.
- Chow VT. 1959. *Open channel hydraulics*. McGraw-Hill: New York; 680.
- Dabney SM. 2003. Erosion Control, Vegetative. In *Encyclopedia of Water Science*, Stewart BA, Howell TA (eds). Marcel Dekker: New York; 209–213.
- Dabney SM, McGregor KC, Wilson GV, Cullum RF. 2009. How management of grass hedges affects their erosion reduction potential. *Soil Science Society of America Journal* **73**: 241–254.
- Dabney SM, Wilson GV, McGregor KC, Vieira DAN. 2011. Runoff through and upslope of contour switchgrass hedges. *Soil Science Society of America Journal*. DOI:10.2136/sssaj2011.0019.
- Defina A. 2000. Two-dimensional shallow flow equations for partially dry areas. *Water Resources Research* **36**: 3251–3264.
- Di Giammarco P, Todini E, Lamberti P. 1996. A conservative finite elements approach to overland flow: the control volume finite element formulation. *Journal of Hydrology* **175**: 267–291.
- Ghidey F, Alberts EE, Kramer LA. 2001. Comparison of measured and WEPP predicted runoff and sediment loss from deep loess soils watershed. In *Soil Erosion Research for the 21st Century: Proceedings of the International Symposium, 3–5 January, 2001, Honolulu, Hawaii, USA*, Ascough II JC, Flanagan DC (eds). American Society of Agricultural Engineers: St. Joseph; 131–134.
- Gilley JE, Kottwitz ER, Wieman GA. 1991. Roughness Coefficients for Selected Residue Materials. *Journal of Irrigation and Drainage Engineering* **117**: 503–514.
- Gilley JE, Kottwitz ER. 1993. Darcy-Weisbach roughness coefficients for selected crops. *Transactions of ASAE* **37**: 467–471.
- Gottardi G, Venutelli M. 1993. A control-volume finite-element model for two-dimensional overland flow. *Advances in Water Resources* **16**: 277–284.
- Lal AMW, Wang N, Moustafa MZ, Brown MC. 2010. Mass residuals in implicit finite volume models for overland and groundwater flow. *Journal of Hydrology* **384**: 26–32.
- Liu QQ, Chen L, Li JC, Singh VP. 2004. Two-dimensional kinematic wave model of overland-flow. *Journal of Hydrology* **291**: 28–41.
- Meyer LD, Dabney SM, Harmon WC. 1995. Sediment-trapping effectiveness of stiff-grass hedges. *Transactions of ASAE* **38**: 809–815.
- Molling CC, Strikwerda JC, Norman JM, Rodgers CA, Wayne R, Morgan CL, Diak GR, Mecikalski JR. 2005. Distributed runoff formulation designed for a precision agricultural landscape modeling system. *Journal of the American Water Resources Association* **41**: 1289–1313.
- Rachman A, Anderson SH, Alberts EE, Thompson AL, Gantzer CJ. 2008. Predicting runoff and sediment yield from a stiff-stemmed grass hedge system for a small watershed. *Transactions of the ASABE* **51**: 425–432.
- Stone, HL. 1968. Iterative solution of implicit approximations of multidimensional partial differential equations. *SIAM Journal on Numerical Analysis* **5**: 530–558.
- Strelkoff TS, Tamimi AH, Clemmens AJ. 2003. Two-dimensional basin flow with irregular bottom configuration. *Journal of Irrigation and Drainage Engineering* **129**: 391–401.
- Tayfur G, Kavvas ML, Govindaraju RS, Storm DE. 1993. Applicability of St. Venant equations for two-dimensional overland flows over rough infiltrating surfaces. *Journal of Hydraulic Engineering* **119**: 51–63.
- Temple DM, Dabney SM. 2001. Hydraulic performance testing of stiff grass hedges. *Proceedings of the Seventh Interagency Sedimentation Conference* **2**: 118–124.
- Temple DM, Robinson KM, Ahring RM, Davis AG. 1987. *Stability design of grass-lined open channels*. Agricultural Handbook 667. U.S. Department of Agriculture, Agricultural Research Service: Washington.
- Vieira JHD. 1983. Conditions governing the use of approximations for the Saint-Venant equations for shallow surface water flow. *Journal of Hydrology* **60**: 43–58.
- Vieira DAN, Dabney SM. 2011. Modeling edge effects of tillage erosion. *Soil and Tillage Research* **111**: 197–207.
- Wilson CG, Matisoff G, Whiting PJ. 2003. Short-term erosion rates from a ⁷Be inventory balance. *Earth Surface Processes and Landforms* **28**: 967–977.
- Wu W, Wang SSY. 2004. Depth-averaged numerical modeling of flow and sediment transport in open channels with vegetation. In *Riparian Vegetation and Fluvial Morphology*. Bennett SJ, Simon A. (eds). American Geophysical Union: Washington; 253–265.